Ann. Rev. Fluid Mech. 1988. 20 : 61–87

FLUID MODELS OF GEOLOGICAL HOTSPOTS

John A. Whitehead

Department of Physical Oceanography, Woods Hole Oceanographic Institution, Woods Hole, Massachusetts 02543

1. INTRODUCTION

Plate tectonics has provided a framework for understanding the motion of the large lithospheric blocks (plates) that make up the surface of the Earth. Many large-scale features of the Earth are now known to result from the movements and interactions of these plates. However, some prominent surface features cannot be directly explained by plate tectonics—in particular, the existence of linear island and seamount chains. Wilson (1963) suggested that these chains, such as Hawaii, were formed as the plates passed over fixed regions of the mantle where large amounts of magma (or at least heat) were being produced. These hotspots are long-living sources of volcanoes. They often display "tracks" of previous episodes elsewhere on the plates (Figure 1). The central concept in explaining hotspots is that their ultimate source is below the region of large lateral flow in the mantle. The surface manifestations of hotspots remain fixed with respect to each other (Morgan 1971), or at most move with relative velocities that are almost an order of magnitude (<2 cm yr^{-1}) less than the plate motions (<15 cm yr^{-1}).

Other features of hotspots give some clues about their size, shape, and duration, but it is safe to say that all evidence is indirect and inconclusive. The ultimate source may be plumes of hot material rising from the core-mantle boundary (Morgan 1971, 1972, Whitehead & Luther 1975, Loper & Stacey 1983). This is consistent with evidence that the D'' zone (from seismic data), which lies above the core-mantle interface, may be dynamically unstable (Stacey & Loper 1983). However, there are other seismically detected layers within the mantle, most notably the layer at 650 km depth,

0066-4189/88/0115-0061$02.00

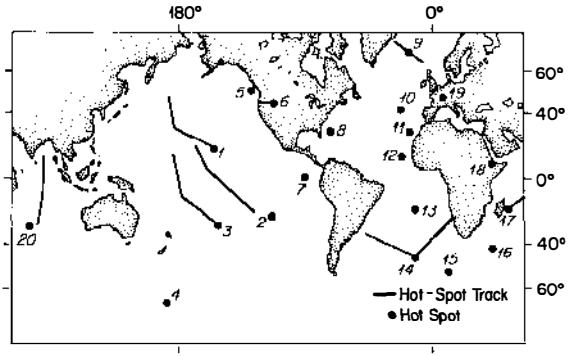

Figure 1 Prominent hotspots of the Earth. The geographic features that define their "tracks" are shown as bold curves and are parenthesized below: 1. Hawaii (Hawaiian Island–Emperor Seamount chain); 2. Easter Island (Sala y Gomez–Nazca Ridge and Tuomoto–Line Island chain); 3. Macdonald Seamount (Austral–Gilbert–Marshall Island chain); 4. Bellany Island; 5. Cobb Seamount (Juan de Fuca Ridge); 6. Yellowstone (Snake River Plain–Columbia Plateau); 7. Galapagos Islands; 8. Bermuda; 9. Iceland; 10. Azores; 11. Canary Islands; 12. Cape Verde Islands; 13. St. Helena; 14. Tristan da Cunha (Rio Grande Ridge, westward; Walvis Ridge, eastward); 15. Bouvet Island; 16. Prince Edward Island; 17. Reunion Island (Mauritius Plateau and Chagos–Laccadive Ridge); 18. Afar; 19. Eifel (Carpathian Mountains); 20. Amsterdam Island–Kerguelen (Ninety-East Ridge) (after Olson & Singer 1985).

that could be dynamically unstable to either heat or material transport (McKenzie & Weiss 1975).

Plumes may have a small cross-section, because there is clear isotopic evidence (O'Nions et al. 1979, 1980) that the melt that forms from hotspot islands has long ago differentiated from the melt that upwells at spreading centers. No evidence of hotspot material is found at spreading centers, even when they override old hotspot locations.

On the other hand, plumes may be wide, since they also produce a broad (order 1000 km) region of uplifted ocean floor around hotspot island chains (Crough 1978). There appears to be a broad-scale reheating of the underside of the plate above hotspots, since the rises in the seafloor are accompanied by a density deficiency that is determined from gravity studies to be at 40 to 100 km depth. However, the uplifted area does not extend ahead of the hotspot by scales of order 1000 km. Instead, the extension ahead is confined to a steep "nose" region. This is consistent with a narrow hotspot that spreads out melting material in the asthenosphere below island chains. It is also consistent with a wide hotspot that is in thermal contact with the base of the plate (Von Herzen et al. 1982).

In any event, fluid models of thermals in low-Reynolds-number fluids [the term "creeping plumes" has been coined by Olson & Singer (1985)]

are extremely useful as models of what may occur within the mantle of our Earth. In this review, we first investigate the flow of convection. Then we discuss studies of the bottom boundary layer, followed by an examination of work on plumes and conduits (plumes of very low viscosity material). In the last section, we summarize studies of the top boundary layers of plumes.

2. CONVECTION

Convection With Constant Viscosity

Flow patterns in thermal convection of constant-viscosity fluid between two horizontal boundaries are among the most extensively studied structures in fluid dynamics. Convection is characterized by two dimensionless numbers—the Rayleigh and Prandtl numbers

$$R_a = \frac{g\alpha L^3 \Delta T}{\kappa \nu}, \qquad P_r = \frac{\nu}{\kappa},$$

where g is the acceleration due to gravity, α is the coefficient of thermal expansion, L is the depth of the fluid, ΔT is the temperature difference between the top and bottom of the fluid, κ is the thermal diffusivity, and ν is the kinematic viscosity. Estimates of R_a for the mantle of the Earth range from 10^4 to 10^7, and this span of 10^3 is principally due to the question of whether whole-mantle or layered convection exists. Mantle values for the Prandtl number are huge, 10^{15} or more. Laboratory studies of large-Prandtl-number convection in a planar layer reveal that the sequence of convection structures encountered at progressively greater R_a are (Krishnamurti 1970, Busse & Whitehead 1971, 1974, Whitehead & Chan 1976, Whitehead & Parsons 1978)

$0 < R_a < 1707$	No motion,
$1707 < R_a \lesssim 21{,}000$	Convection rolls,
$21{,}000 < R_a < 50{,}000$	Bimodal flow (two rolls at right angles),
$50{,}000 \lesssim R_a < ?$	Spoke convection (which sometimes oscillates),
$150{,}000 \lesssim R_a < 10^6$	Squares.

The value of R_a at which motion starts is usually called the critical Rayleigh number. We denote it as R_c in this article. Photographs of the different

flows are shown in Figure 2. Laboratory experiments show that spoke convection in fluids with Prandtl numbers up to 10^4 exhibits time-dependent oscillations whose dynamical origin is believed to be linked to inertial terms in the Navier-Stokes equations. If the inertial terms are central, the large Prandtl number appropriate for the mantle may imply the absence

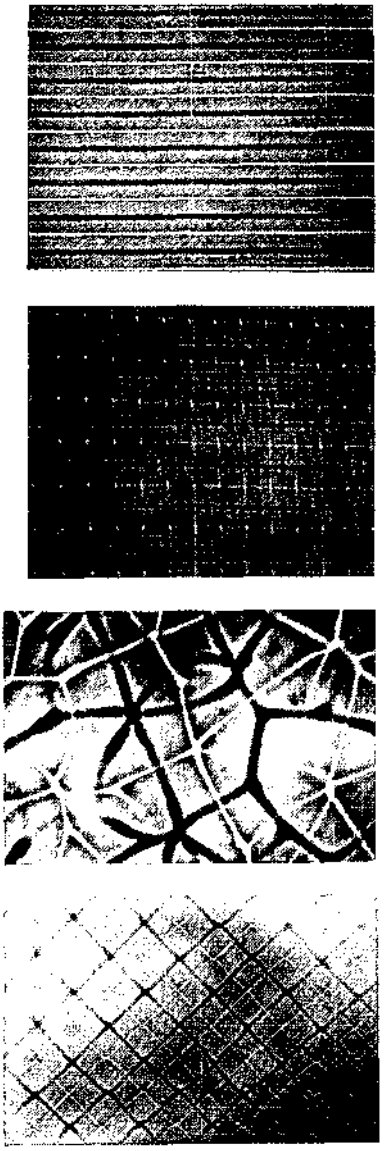

Figure 2 Four of the structures observed in high-Prandtl-number convection with constant viscosity. From top to bottom, respectively, are rolls, bimodal flow, spoke convection, and squares. The latter break down to spokes in the presence of dislocations.

of oscillations. The squares are unlikely to be seen in convection that arises from random initial conditions, because squares break down to spokes in the presence of dislocations.

Richter & Parsons (1975; see Richter 1978a) have shown that when these flows are subjected to shear, they revert to rolls aligned with the shear, even if the original flow is bimodal or spokes. This led these authors to suggest that convection rolls may be expected under plates, with the rolls aligned at right angles to the direction of plate motion with respect to the hotspot frame.

The planforms appropriate for a spherical Earth differ significantly from the roll patterns that appear for planar convection in an isoviscous fluid. Figure 3 shows the pattern of convection predicted by Busse (1975, 1979) for convection close to R_c. This example exhibits tetrahedronal symmetry, corresponding to the spherical harmonic $l = 6$. Lines of constant radial velocity are drawn, and the flow can go either up or down in the shaded regions. The analysis indicates that even values of the harmonics are preferred over odd values. There is no evidence for the preference of even over odd harmonics in the gravity field of the Earth nor in the recent tomographic inversions of travel time through the mantle of the Earth.

Convection With Viscosity Variation

An important advance in the theoretical understanding of pattern selection by convection came from analysis of convection with temperature-dependent properties. Palm (1960), Segel & Stuart (1962), and Busse (1962, 1967) found that the hexagonal planform played a key roll in the finite-amplitude instability of convection in the vicinity of R_c, and that only hexagons of one sign would be preferred. In the case of a fluid whose viscosity is lowered with increasing temperature (such as the mantle of the Earth),

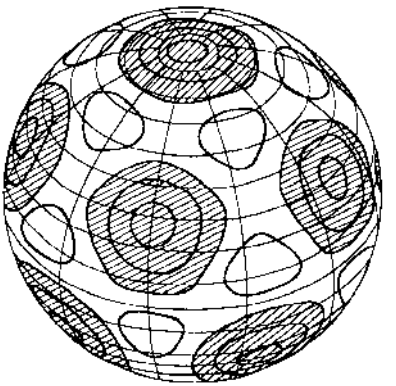

Figure 3 One possible planform of convection on a sphere from Busse (1975). This pattern corresponds to tetrahedronal symmetry, corresponding to the spherical harmonic $l = 6$. Vertical velocity contours are shown, and flow can go either up or down in the crosshatched region for convection with uniform viscosity.

hexagons with centers of rising fluid are anticipated. Each center is surrounded by a descending hexagonal region of colder (and more viscous) fluid. At higher values of R_a, the hexagons give way to rolls. Figure 4 shows a shadowgraph of such a hexagonal pattern near R_c in glycerin. It is found in practice that other polygons are possible near dislocations in the hexagonal matrix, yet the polygons retain a central feature of hexagonal symmetry, which is that all "hexagons" consist of connected, cold (white) boundary layers and unconnected, hot (black) boundary layers. Stuart (1964) discussed the asymmetry between connected and unconnected regions. Booker (1976), Oliver (1980), Oliver & Booker (1983), Richter (1978b), and White (1982) have conducted extensive laboratory experiments with fluids of large viscosity variation in which the hexagonal, roll, or square convection patterns are found. Figure 5 summarizes the observations of Oliver & Booker (1983). In cases where the viscosity variation is enormous, the square pattern most strongly localizes the ascending flow into cylindrical hot thermals of low viscosity, with the surrounding fluid sinking as viscous colder material. The cells are capped by a thick, cold, viscous boundary layer that confines vertical penetration of the thermal to the bottom portion of the convecting fluid.

Studies of convection have been limited by numerous practical problems. Analysis of convection is very useful and powerful for predicting planforms and transport rates but is effectively limited to parameter regions close to R_c. Analytical methods can be coupled with numerical treatments of the mode interactions to extend the range of calculations by factors of 10 to 100 above R_c. These methods have been used to complete studies of the stability of hexagons, rolls, and squares in the large-Prandtl-number limit. Busse & Frick (1985) have shown analytically that squares become stable when viscosity variation is sufficiently great. Even though thermal convection is the most extensively studied class of flow structures driven by

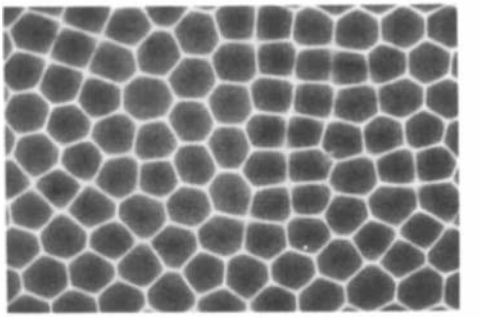

Figure 4 Shadowgraph of a polygonal flow pattern in glycerin close to the critical Rayleigh number. Most of the cells are hexagonal, but there are some pentagons and squares.

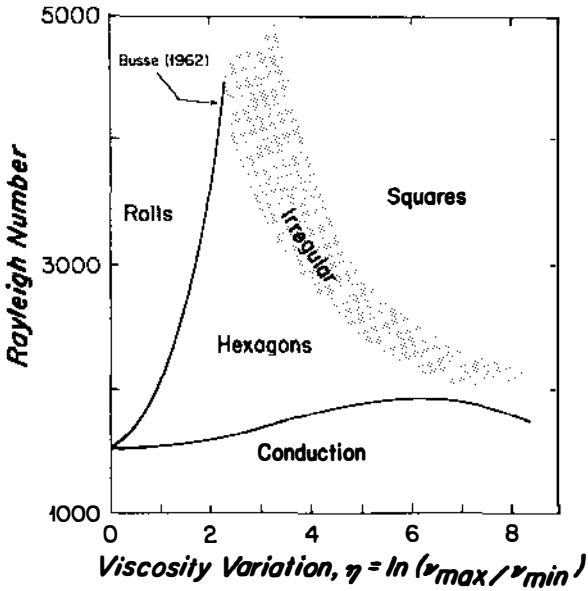

Figure 5 The different stability regions of convection planforms as observed by Oliver & Booker (1983). The squares are not to be confused with the constant-viscosity squares in Figure 2.

upward heat flux, it may not be the simplest model of mantle plumes. To show why, we next resort to some scaling considerations.

3. THE BOTTOM BOUNDARY LAYER

Scaling

Using the following scalings for velocity, temperature, and time,

$$\frac{\kappa}{L}, \qquad \Delta T, \qquad \frac{L^2}{\kappa},$$

we can derive the following dimensionless continuity, Navier-Stokes, and heat equations:

$$\nabla \cdot \mathbf{u}_n = 0,$$

$$P_r^{-1} \frac{D\mathbf{u}_n}{Dt} = -\nabla p + \nabla^2 \mathbf{u}_n + R_a T_n \hat{\mathbf{k}},$$

$$\frac{DT_n}{Dt} = \nabla^2 T_n,$$

where D denotes a total derivative.

In applying these equations to the mantle of the Earth, one must realize that numerous important physical features are missing from them. Probably the largest omission involves the variation of viscosity with temperature, pressure, and perhaps composition. Since the surface manifestation of hotspot volcanism is fully melted material (magma), viscosity contrasts between the mantle and hotspot material may be enormous! Two other missing features are the absorption of latent heat by melting and the thermodynamic effect of the large pressure differences between the top and base of the mantle. (The mantle depth is a sizable fraction of an adiabatic scale height.) These effects have been incorporated in numerous studies of special problems, some of which are discussed in later sections.

What are the sizes of the dimensionless Prandtl and Rayleigh numbers in the Earth's mantle? Viscosity ν is of order 10^{20} cm^2 s^{-1}, thermal diffusivity κ is of order 10^{-2} cm^2 s^{-1}, $\alpha \nabla T$ is of order 10^{-1}, and L is of order 10^8 cm. These numbers lead to $P_r \approx 10^{22}$ and $R_a \approx 10^8$. The Prandtl number is sufficiently large that the inertial terms on the left-hand side of the Navier-Stokes equation may always be left out, but the Rayleigh number is so large that the starting velocity and time scales are unrealistic. For instance, κ/L is 10^{-10} cm s^{-1}, whereas plate drift motion is of order 10^{-6} cm s^{-1}. Surely vertical motions associated with hotspots would be even greater. Also, the time scale L^2/κ is 10^{18} s, whereas the age of the Earth is of order 10^{17} s. In spite of these discrepancies, numerous convection studies have been made starting from the above equations. Velocities end up being scaled by R_a^n, where n ranges between 1/4 and 1. For purposes of this review, a more direct scaling for velocity and time is

$$\frac{R_a \kappa}{L}, \qquad \frac{L^2}{R_a \kappa}.$$

Using the above numbers, we get a velocity scale of 10^{-2} cm s^{-1} and a time scale of 10^{10} s.

These lead to the following dimensionless equations:

$$\nabla \cdot \mathbf{u} = 0,$$

$$R_a P_r^{-1} \frac{D\mathbf{u}}{Dt} = -\nabla p + \nabla^2 \mathbf{u} + T\hat{\mathbf{k}},$$

$$\frac{DT}{Dt} = R_a^{-1} \nabla^2 T.$$

Inertia can still safely be neglected, but in addition the thermal-conduction term on the right side of the heat equation can be neglected to the lowest order approximation. Only corrections of order R_a^{-1} will involve the redistribution of heat due to thermal conductivity. In the next two sections, we review problems in which both inertia and thermal conduction are neglected.

Gravitational Instability of the Bottom Boundary Layer

The initiation of plumes must clearly begin with the formation of upwelling regions. One approach is to investigate the gravitational instability of a horizontal layer of fluid lying under a denser layer of fluid. The lower layer will then develop Rayleigh-Taylor instability. The wavelength of maximum growth rate and the exponential time constant of growth have been theoretically and numerically predicted for a number of geometries and boundary conditions (Rayleigh 1900, Dobrin 1941, Chandrasekhar 1955, Daněs 1964, Selig 1965, Ramberg 1963, 1967a, 1968a,b,c, 1970, Biot 1966, Biot & Ode 1965, Berner et al. 1972, Whitehead & Luther 1975, Marsh 1979, Whitehead et al. 1984). Demonstration experiments with putty and other non-Newtonian fluids have been extensively photographed and compared with geological formations by Nettleton (1934, 1943), Parker & McDowell (1955), and Ramberg (1963, 1967b, 1970). There was no intercomparison between the laboratory experiments and theory due to the unknown rheology of the laboratory materials.

The limit in which one layer is thin and of lower viscosity than the other is particularly relevant in the geophysical context. Take the configuration shown in Figure 6, in which a thin layer of density $\rho - \Delta\rho$, depth d, and viscosity μ_1 lies under a semi-infinite fluid of density ρ and viscosity μ_2. Let the wavelength l of the disturbance $\eta(x, t)$ to the horizontal interface be larger than the depth d of the thin layer, so that the lateral velocity u in the thin layer is larger than the vertical velocity. The scaling argument used here can be found in a number of the cited studies. The force balance is between the lateral pressure gradient p/l and viscosity, and thus we have

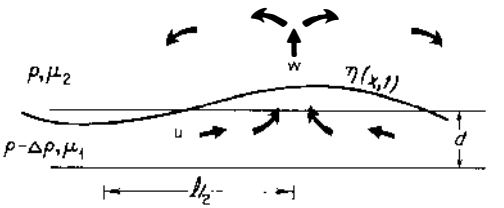

Figure 6 Definition parameters for the analysis of Rayleigh-Taylor instability of a thin layer lying under a deep fluid.

$$\frac{p}{l} = \mu_1 \frac{u}{d^2}. \tag{1}$$

In the deep viscous fluid that lies overhead, the force balance is between stress due to the vertical velocity w of the interface, pressure, and buoyancy, which gives us

$$\frac{p}{l} = \mu_2 \frac{w}{l^2} + \frac{g\Delta\rho\eta}{l}. \tag{2}$$

Combining (1) and (2), we have

$$\mu_1 \frac{u}{d^2} - \mu_2 \frac{w}{l^2} = \frac{g\Delta\rho\eta}{l}. \tag{3}$$

Using continuity

$$\frac{u}{l} + \frac{w}{d} = 0, \tag{4}$$

kinematics of the interface

$$\frac{\partial\eta}{\partial t} = w, \tag{5}$$

and the fact that the growth will be exponential ($w = w_0 e^{\sigma t}$), we find that

$$\sigma = \frac{g\Delta\rho}{\mu_2} \frac{l}{\frac{\mu_1}{\mu_2}\frac{l^3}{d^3} + 1}. \tag{6}$$

The growth rate σ is shown as a function of the normalized wavelength l/d in Figure 7. Note that the maximum growth occurs at

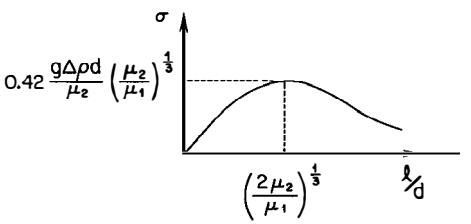

Figure 7 Growth rate as a function of wavelength for one layer undergoing Rayleigh-Taylor instability.

$$\frac{l}{d} = \left(\frac{2\mu_2}{\mu_1}\right)^{1/3} = 1.26\left(\frac{\mu_2}{\mu_1}\right)^{1/3}, \tag{7}$$

where the growth rate is

$$\sigma = 0.42\left(\frac{g\Delta\rho d}{\mu_2}\right)\left(\frac{\mu_2}{\mu_1}\right)^{1/3}. \tag{8}$$

The central finding here is that the fastest growth length scale is proportional to $(\mu_2/\mu_1)^{1/3}$ (which may be a large number). Two superior (but larger) calculations using the complete hydrodynamics equations have been made that also show this. The wavelength l of fastest growth is found by Whitehead & Luther (1975) for a free-slip boundary condition to be

$$\frac{l}{d} = 4.36\left(\frac{\mu_2}{\mu_1}\right)^{1/3}, \tag{9}$$

where the growth rate is

$$\sigma = 0.232\left(\frac{g\Delta\rho d}{\mu_2}\right)\left(\frac{\mu_2}{\mu_1}\right)^{1/3}. \tag{10}$$

Selig (1965) [his equations (2.11)] has found that if the thin layer has a no-slip lower boundary condition, then

$$\frac{l}{d} = 2.9\left(\frac{\mu_2}{\mu_1}\right)^{1/3} \tag{11}$$

and

$$\sigma = 0.153\left(\frac{g\Delta\rho d}{\mu_2}\right)\left(\frac{\mu_2}{\mu_1}\right)^{1/3}. \tag{12}$$

The wavelength prediction has been tested in an experiment by Whitehead & Luther (1975) that is shown in Figure 8. The thin layer of dyed fluid was lower in viscosity than the deep transparent fluid. In this case, four or five regularly spaced protrusions developed shortly after the experiment started. The protrusions also arranged themselves quite uniformly throughout the tank. The normalized wavelength predicted by Equation (11) for the experiment shown in Figure 8 is 10.1, which agrees quite well with the observation.

Physically, a horizontal layer of relatively low-viscosity fluid develops a long-wavelength disturbance because it is more efficient for the low-viscosity fluid to flow large, lateral distances up a gradual slope and to

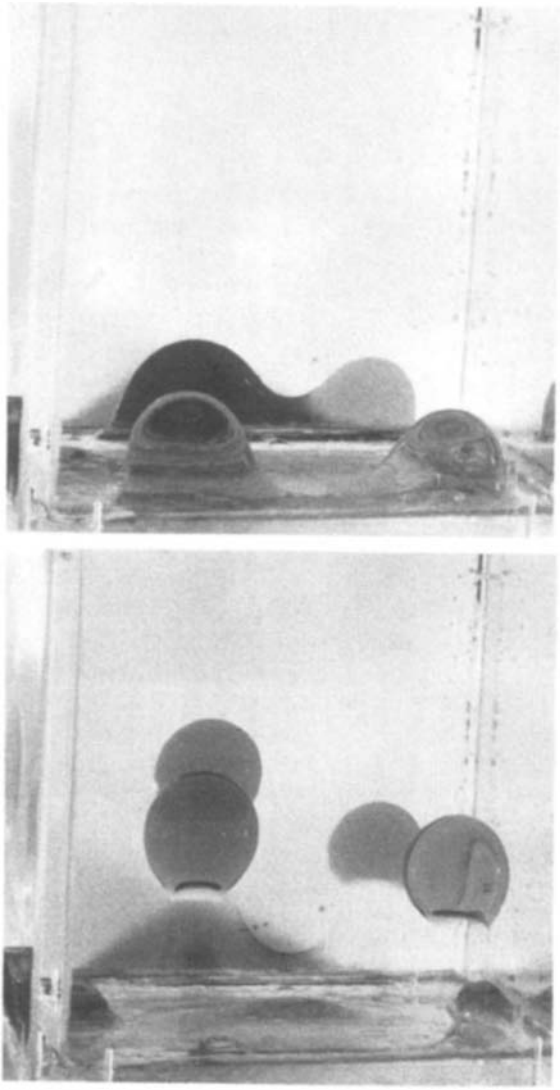

Figure 8 An experimental demonstration of Rayleigh-Taylor instability.

accumulate in massive upwellings. These have more force with which to intrude up into the very viscous, stiff overlying material than do the diapirs (upwelling geological structures) formed by shorter wavelength instabilities. Salt domes are a vivid geological example of the accumulation of low-viscosity material over large lateral distances. They are sometimes hundreds of meters deep and thick, yet appear to have originated by depleting a 10-m-thick salt stratum over distances of thousands of meters (Nettleton 1934, 1943, Braunstein & O'Brien 1968).

The stability of a hot bottom boundary layer in a gravitational field with strongly temperature-dependent viscosity has been investigated by Jackson & Talbot (1986), Yuen & Peltier (1980a), and Stacey & Loper (1983). Yuen & Peltier (1980a) recovered narrow boundary-layer modes in the thermal field, but they found that the velocity field is still not largely confined to the hot viscous region. They used this result to reject the concept of localized plumes arising from a low-viscosity boundary layer at the base of the mantle. Loper & Stacey (1983) attributed their failure to find narrow plumes to a viscosity contrast that was set too small. For larger values, they did find very narrow plumes. Hence, they have strongly readvocated the concept of a low-viscosity boundary layer at the base of the mantle.

4. PLUMES AND CONDUITS

Constant Viscosity

For practical calculations of the sizes, speeds, and other features of hotspots, numerous studies have been conducted that focus on the rising, hot, axisymmetric (or "plume") portion of the cell. Indeed, it is not clear in the mantle context that the cold, viscous, polygonal sinking portions of thermal-convection cells have any direct connection to the Earth's cold, rigid, sliding tectonic plates.

Parmentier et al. (1976) numerically integrated the axisymmetric equations of motion for internally heated and base-heated fluids with either variable or fixed viscosity. For constant viscosity, the ascending limb of the convection cell was wide and diffuse [Figure 9 (*left*)]. However, the situation may be different for hotspots with a constant-viscosity mantle.

Olson & Singer (1985) have modeled the start-up of a constant-viscosity plume as a constantly growing buoyant cylinder. The low-Reynolds-number terminal velocity w of a vertical cylinder having length L, density $\rho-\Delta\rho$, and radius r in fluid with kinematic viscosity ν and density ρ is

$$w = b\frac{g^* r^2}{\nu}\ln\frac{L}{r}, \tag{13}$$

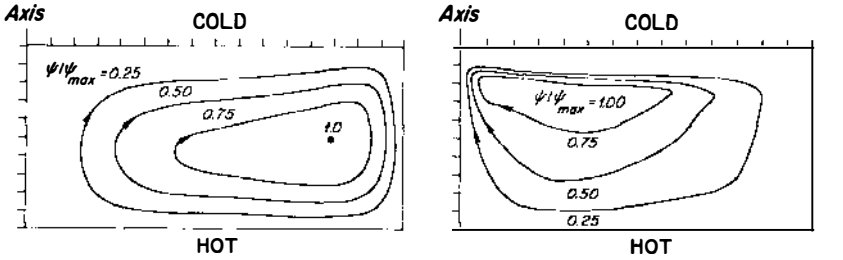

Figure 9 Streamlines from calculations by Parmentier et al. (1976) for an axisymmetric cell of fluid heated from below with a constant-viscosity (*left*) and variable-viscosity fluid (*right*). In the latter case, the upwelling concentrates into a round jet. The stream function is normalized with respect to its maximum value.

where $g^* = g\Delta\rho/\rho$ is called reduced gravity, and b is a proportionality factor that they find to be approximately one.

If the cylinder grows from a steady-state volume flux Q, then we have

$$\frac{dL}{dt} = w \tag{14}$$

and

$$\frac{d}{dt}\pi r^2 L = Q. \tag{15}$$

Equations (13)–(15) can be rearranged to give

$$\frac{dL}{dt} = \frac{bg^* r^2}{\nu} \ln\frac{L}{r}, \tag{16}$$

$$\frac{dr}{dt} = \frac{Q}{2\pi r L} - b\frac{g^* r^3}{2\nu L} \ln\frac{L}{r}. \tag{17}$$

Olson & Singer (1985) integrated Equations (16) and (17) and used as a starting radius r_0, the root of the right-hand side of (17), or

$$r_0^4 \ln\left(\frac{L_0}{r_0}\right) = \frac{\nu Q}{\pi b g^*}. \tag{18}$$

The solutions fit their data well with a coefficient $b = 1$. Their Figure 4 reveals that the cylinder initially grows rapidly, but it soon reaches a state where the radius grows very slowly. In this case the right-hand side of (17) is almost perfectly zero and thus

$$Q = \frac{\pi b g^* r^4}{\nu} \ln \frac{L}{r}. \tag{19}$$

It then follows that

$$\frac{dL}{dt} = (\pi r^2)^{-1} Q \tag{20}$$

or, using (19), that

$$\frac{dL}{dt} = \left(\frac{\pi \nu}{b g^* \ln \frac{L}{r}} \right)^{1/2} Q^{3/2}, \tag{21}$$

which is almost a constant in time for steady Q, given the slow variation of the function $(\ln L/r)^{1/2}$ with L/r.

Plumes With Variable Viscosity

Parmentier et al. (1976) numerically calculated the flow fields in a cylindrical cell of fluid heated uniformly from below. For a constant-viscosity fluid, the areas of upwelling and downwelling fluids were roughly equal. For a variable-viscosity fluid, the upwelling streamlines dramatically pinched together. Figure 9 (*right*) shows the streamlines from one solution in which the viscosity varied by approximately 10^5, and this can be compared with the equivalent calculation [Figure 9 (*left*)] for constant-viscosity fluid. In the constant-viscosity case, the upwelling area was wide and diffuse; in the variable-viscosity case, the upwelling concentrated in a lubricated jet.

Whitehead & Luther (1975) discovered that low-viscosity material injected into the base of higher viscosity material will rise as a sphere, followed by a very small plume, or conduit (Figure 10). The conduit adopts a radius

$$r_0 = \left(\frac{8 \nu_1 Q}{\pi g^*} \right)^{1/4}, \tag{22}$$

where ν_1 is the viscosity of the low-viscosity material. The velocity distribution $w(r)$ of the fluid in the conduit follows the laminar pipe-flow formula

$$w = \frac{1}{4\nu_1} g^* (r_0^2 - r^2), \tag{23}$$

and the average velocity is

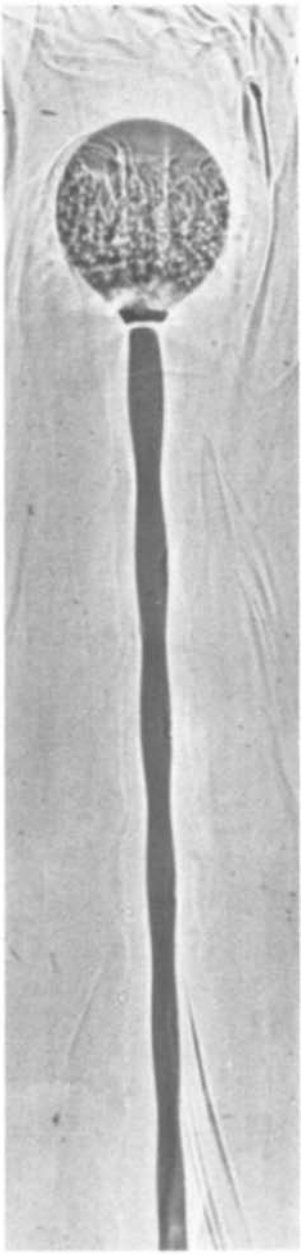

Figure 10 An initiating upwelling sphere trailed by a conduit of rising fluid, as discovered by Whitehead & Luther (1975).

$$\bar{w} = \frac{g^* r_0^2}{8\nu_1}, \tag{24a}$$

or, using (22),

$$\bar{w} = \left(\frac{g^* Q}{8\pi\nu_1}\right)^{1/2}. \tag{24b}$$

The radius r_s of a sphere grows from zero as a point source is turned on. Initially, it obeys the conservation-of-mass law

$$4\pi r_s^2 \frac{dr_s}{dt} = Q, \tag{25}$$

which for constant Q integrates to

$$r_s = \left(\frac{3Qt}{4\pi}\right)^{1/3}. \tag{26}$$

Using the Stokes law for the speed of ascent of a sphere of radius r_s, we have

$$w_s = \frac{1}{3}\frac{r_s^2 g^*}{\nu_2}\left(\frac{\nu_2 + \nu_1}{\nu_2 + \frac{3}{2}\nu_1}\right), \tag{27}$$

where ν_2 is the viscosity of the outer fluid. Using $\nu_2 \gg \nu_1$, we find that the rate of ascent of the sphere is

$$w_s = \frac{1}{3}\frac{g^*}{\nu_2}\left(\frac{3Qt}{4\pi}\right)^{2/3}. \tag{28}$$

As the sphere rises, it must continue to be fed by the fluid coming up the trailing conduit. This begins to slow the growth of the sphere as the rate of the sphere rise approaches the average velocity of the fluid rising in the conduit. Olson & Singer (1985) have predicted and confirmed that at "intermediate" times the rate of ascent is

$$w_s = 0.225\left(\frac{g^*}{\nu_2}\right)^{4/5} Q^{3/5} t^{2/5}. \tag{29}$$

Whitehead & Luther (1975) predict that at very long times, i.e.

$$t \gg 4\left[\frac{\pi\nu_2^6}{g^{*3} Q \nu_1^3}\right]^{1/4}, \tag{30}$$

the sphere will rise with the average velocity of fluid in the conduit, and the equation for the radius of the sphere during this asymptotic time can be found by equating the Stokes solution for the rate of rise of a sphere (27) (assume $\nu_2 \gg \nu_1$) with the relation for average velocity in the conduit (24b). This gives

$$r_s = \left(\frac{9Q\nu_2^2}{8\pi g^* \nu_1}\right)^{1/2}, \tag{31}$$

for which the speed is then found from (28) to be

$$w_s = \left(\frac{g^* Q}{8\pi \nu_1}\right)^{1/2}. \tag{32}$$

Note that this speed is independent of the viscosity of the outer fluid.

The above formulas for the sizes and velocities of conduits and spheres constrain the values of viscosity, density, and volume flux within the Earth if these structures are to exist. Such considerations have been widely used (Olson & Singer 1985, Epp 1984, Crough 1978, Stacey 1977, Loper & Stacey 1983, Schouten et al. 1985, Whitehead & Luther 1975, Skilbeck & Whitehead 1978, Whitehead 1982).

The equivalent of these conduits and spheres when thermal diffusivity and temperature-dependent viscosity are included have also been analyzed. The equivalent of the conduit has been analyzed by Yuen & Schubert (1976) and Yuen & Peltier (1980b), who were forced to prescribe a constant-temperature core to the conduit (equivalent to a heat source distributed through the vertical at $r = 0$). Loper & Stacey (1983) were able to generate conduit solutions by employing an exponential viscosity-temperature relation, which in practice made viscosity vary greatly with temperature. Not only is their "chimney" narrow given the sensitivity of viscosity with temperature, but it also develops a small radial inflow of the outer cold fluid that keeps the thermal field trapped to the chimney radius. Oliver (1980) had found such a process in generating a similarity solution for a two-dimensional vertical sheet with temperature-dependent viscosity but was unsuccessful at generating a similarity solution for a conduit, or chimney. Boss & Sacks (1985) have conducted numerical experiments for two-dimensional sheets of low-viscosity fluid. However, sheets do not appear to be realized in laboratory experiments.

Skilbeck & Whitehead (1978), Whitehead (1982), and Loper & Stacey (1983) have found that their solutions for the radius of such conduits in the Earth give values of order 10 km, or at most between 1 and 100 km. Such structures are beyond the limits of seismic or electromagnetic

resolution, but such small radius values could explain how hotspot material can remain differentiated from mantle material.

Waves on Conduits

Scott et al. (1986) and Olson & Christensen (1986) have found that the conduits support solitary waves. The wave equation is of the form

$$\frac{\partial A}{\partial t} = -\frac{\partial Q}{\partial z}, \tag{33}$$

$$Q = \frac{A^2}{8\pi v_1}\left[g^* + v_2 \frac{\partial}{\partial z}\frac{1}{A}\frac{\partial Q}{\partial z}\right], \tag{34}$$

where $A = \pi r^2$ is the cross-sectional area of the conduit, Q the volumetric flux up the conduit, z the vertical coordinate, t the time, v_1 the viscosity of the rising fluid, and v_2 the viscosity of the host fluid. Equation (33) is simply a conservation-of-mass relation between the change in cross-sectional area of the conduit and the divergence of the volumetric flux. Equation (34) is closely related to the pipe-flow formula (24a), except that an additional term on the extreme right is added. This term arises as follows: The pressure distribution in the outer fluid obeys Laplace's equation, so it is represented by the modified Bessel function $K_0(kr)$ sin kz, where k is the vertical wave number and r is the radial direction coordinate. In the limit $kr \ll 1$ (long-wavelength limit), the radial flow has the form

$$v_r \approx \frac{1}{r} + O(kr^2 \ln kr). \tag{35}$$

This admits the simplified normal-stress boundary condition

$$p_1 - p_2 + \rho g z = 2v_2 \frac{v_r(r)}{a}. \tag{36}$$

Using $v(r) = \partial r/\partial t$, a modified Equation (23) that is a pressure-driven "pipe-flow law," and Equation (33), we get Equation (34). Olson & Christensen (1986) find two classes of solutions. The first consists of isolated solitary waves. In the large-amplitude limit, their wave solution is

$$A = A_m \exp\left(-\frac{y^2}{2cy_0^2}\right), \tag{37}$$

where

$$c = \frac{2A_m^2 \ln A_m - A_m^2 + 1}{(A_m - 1)^2}, \tag{38}$$

$$y = z - ct, \tag{39}$$

$$y_0 = \left(\frac{\nu_2 A_0}{8\pi\nu_1}\right)^{1/2} \tag{40}$$

is the length scale, and the wave travels with velocity $(g^* A_0/8\pi\nu_2)c$.

The waves possess interesting soliton properties upon collision (Scott et al. 1986, Whitehead 1987), although Barcilon & Richter (1986) find that the waves are not true solitons (to some percent) in numerical experiments. However, Equations (33) and (34) can be reduced to the Korteweg–de Vries equations for solitons in the small finite-amplitude limit (Whitehead & Helfrich 1986). Figure 11 is a temporal sequence of photographs of two very large waves as they collide. A position jump in the trajectory of the two waves is visible, and hence the waves appear superficially to possess soliton properties.

Effect of Shear on Plumes and Conduits

A limited number of studies have been made on the effects of shear on large plumes. Richter & Parsons (1975; see Richter 1978a) suggest that convection cells under the tectonic plates take the form of convection rolls

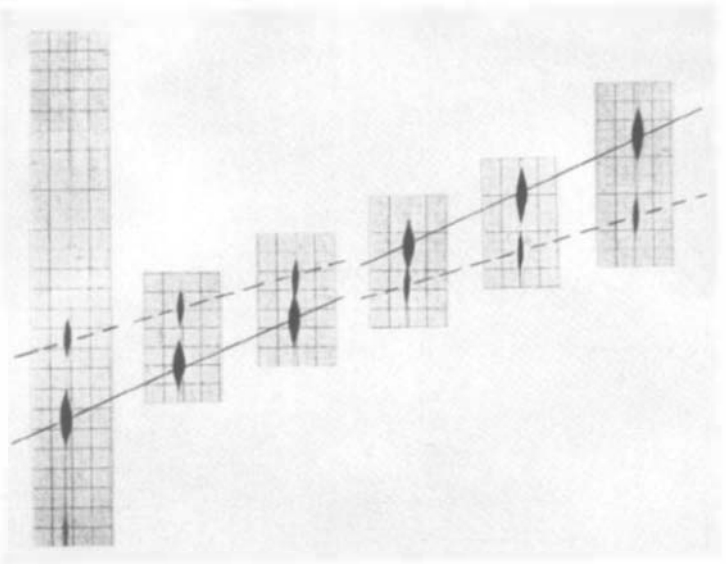

Figure 11 A time sequence with equal time steps of two solitary waves rising through a very tiny conduit, which is not always visible in these photographs. The waves collide and interact like solitons. The position or "phase" jump of each wave is visible.

aligned with shear. This concept is generally applied to the alignment of cold convection thermals from cooling of the lithospheric plates.

It is simple to see that shear under the plates will tilt hotspots enough to generate fluid-dynamical instabilities, but studies of such instabilities are relatively rare. Skilbeck & Whitehead (1978) and Whitehead (1982) have shown that low-viscosity conduits that are tilted by shear to an angle of approximately 30° with the horizontal will develop an instability. This instability has the form of growing waves that break upward. Eventually one wave breaks away from the conduit and initiates a new sphere. The sequence has been documented with analytical, numerical, and laboratory studies. Figure 12 shows two photographs (Whitehead 1982) of a laboratory experiment in which the conduit was tilted by shear in a Hele-Shaw cell. Quantitative estimates of the spacing between cavities suggest that this spacing is largely determined by the depth of the shear zone.

Olson & Singer (1985) have studied the effect of a moving plume source (which is equivalent to a sharp shear layer at some depth in the Earth). They assert that cavity spacing is independent of source discharge, which leads to the relation

$$\frac{W}{U} = 0.55\left[\frac{g^*Q}{\nu_2 U^2}\right]^{1/2}, \tag{41}$$

where W is the upwelling velocity of the spheres, and U is the tow speed. Figure 13 shows laboratory measurements of the angle tangent of a chain of ascending spheres from a towed source.

5. DYNAMICS NEAR THE TOP OF HOTSPOTS

Stagnation Point Problems

There are numerous problems concerning the top of hotspots and the penetration of heat or magma into the plate above hotspots. These are beyond the scope of this article. Such problems include studies of the effects of temperature-dependent viscosity on flow past heated spheres (Morris 1982, Emerman & Turcotte 1983a, Ribe 1983), the behavior of thermals with heat conduction (Griffiths 1986), the spreading of thermals as they stagnate under a plate (Emerman & Turcotte 1983b, Olson & Nam 1986), and the shape of the thermal field in a moving plate due to a hotspot (Von Herzen et al. 1982). In most of these studies, thermal conduction plays a key role in allowing heat or material from the hotspot to penetrate upward through the lithospheric plate. Many other studies incorporate a more complicated rheology than that of Newtonian fluid.

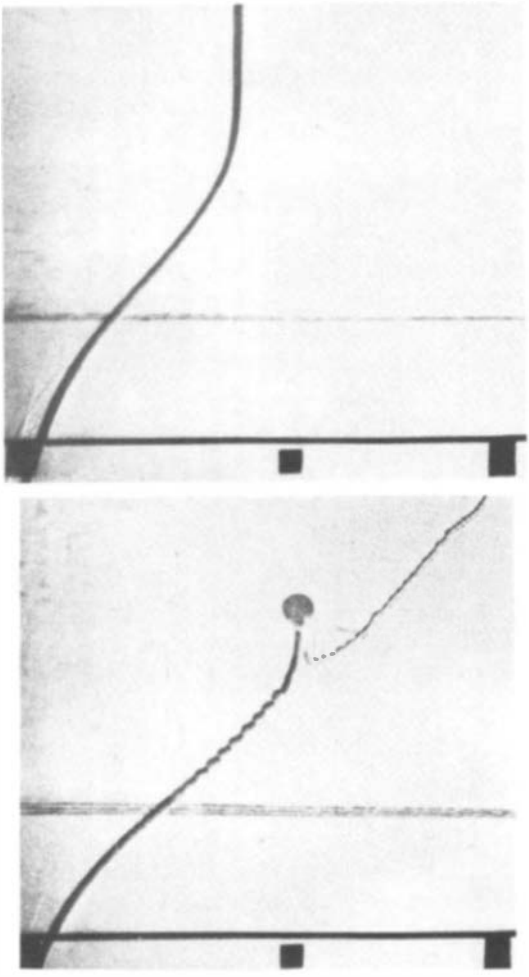

Figure 12 The instability of a conduit that is tilted by shear (Whitehead 1982).

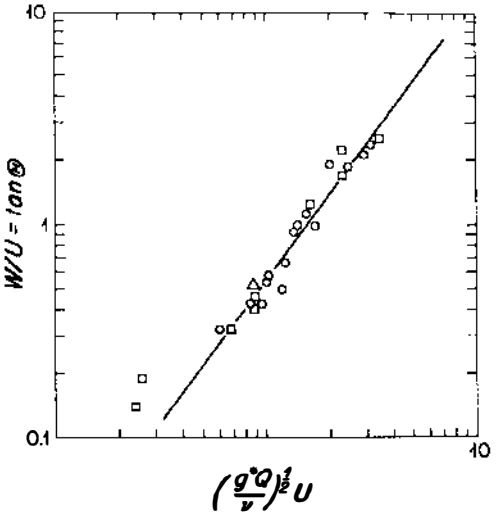

Figure 13 The angle tangent of a train of creeping plumes from a towed source, as observed by Olson & Singer (1985).

The behavior of spherical pockets of hot fluid with temperature-dependent viscosity has been studied by Marsh (1982), Morris (1982), Ribe (1983), and Griffiths (1986). Attention has largely focused upon the thermal interaction between the sphere and its surroundings. The applications are generally to problems where

$$\frac{\kappa t}{L^2} > 1. \tag{42}$$

In order for time scales t to be less than 30 Myr ($t = 10^{15}$ s), we must have $L < 10$ km. Thus this problem usually applies to penetration of magma bodies in the top part of the mantle.

Compaction

Another series of studies have focused on the migration of melt through the mantle material near the top of the hotspot. It is believed that the mantle of the Earth is largely a (creeping) solid. However, as material from deep in the Earth is brought toward the surface, it can cross the solidus curve in pressure-temperature space. When this happens, it is believed that a small percentage of material will melt. Based upon recent measurements (Waff 1980, Cooper & Kohlstedt 1984, Waff & Bulau 1979), it is likely that the melt will interconnect along the grain boundaries and thus will form a porous network. The melt will be out of hydrostatic equilibrium

with the unmelted crystal grains, and it will be forced upward by gravitational compaction of the crystals. The laws governing the flow rates (Fowler 1984, McKenzie 1984, Richter & McKenzie 1984, Scott & Stevenson 1984) are generally somewhat complicated. The dynamics of a flowing compacting medium have been studied by Ribe (1985). In one limit (Scott et al. 1986, Whitehead 1986), the laws are analogous to Equations (33) and (34) for solitary waves in the conduit. In the analogy (which is in one sense more than an analogy, since the dynamics are almost the same), the area A of the conduit is replaced by the porosity of the rock, but all other quantities are the same. Thus simplified compaction flow through porous media resembles the flow of a low-viscosity fluid up a conduit.

Numerical experiments indicate that one-dimensional "waves" of enhanced melt are unstable in two dimensions, and that these go on to form two-dimensional solitary waves (magmons). These take the form of cylinders of enhanced melt rising through the matrix (Scott & Stevenson 1984, 1986, Scott 1987).

ACKNOWLEDGMENTS

Support for research in geological fluid mechanics at Woods Hole Oceanographic Institution is received from the Geodynamics Program of the Institution. Previous research on diapir genesis was supported by the Geophysical Division of the National Science Foundation under grant EAR78-12927. I wish to thank Mr. Robert E. Frazel for the photographic work and Anne-Marie Michael for typing the manuscript.

Literature Cited

Barcilon, V., Richter, F. M. 1986. Nonlinear waves in compacting media. *J. Fluid Mech.* 164: 429–48

Berner, H., Ramberg, H., Stephansson, O. 1972. Diapirism in theory and experiment. *Tectonophysics* 15: 197–218

Biot, M. A. 1966. Three-dimensional gravity instability derived from two-dimensional solutions. *Geophysics* 31: 153–66

Biot, M. A., Ode, H. 1965. Theory of gravity instability with variable over-burden and compaction. *Geophysics* 30: 213–27

Booker, J. R. 1976. Thermal convection with strongly temperature-dependent viscosity. *J. Fluid Mech.* 76: 741–54

Boss, A. P., Sacks, I. S. 1985. Formation and growth of deep mantle plumes. *Geophys. J. R. Astron. Soc.* 80: 241–55

Braunstein, J., O'Brien, G., eds. 1968. *Diapirism and Diapirs, Mem. No. 8.* Tulsa, Okla: Am. Assoc. Pet. Geol.

Busse, F. H. 1962. *Das Stabilitätsverhalten der Zellularkonvektion bei endlicher Amplitude.* PhD thesis. Ludwig-Maximilian Univ., Munich, West Ger. Transl. S. H. Davis, 1966, as *Ref. LT-66-19*, Rand Corp., Santa Monica, Calif.

Busse, F. H. 1967. The stability of finite amplitude cellular convection and its relation to an extremum principle. *J. Fluid Mech.* 30: 625–49

Busse, F. H. 1975. Patterns of convection in spherical shells. *J. Fluid Mech.* 72: 67–85

Busse, F. H. 1979. High Prandtl number convection. *Phys. Earth Planet. Inter.* 19: 149–57

Busse, F. H., Frick, H. 1985. Square-pattern convection in fluids with strongly tem-

perature-dependent viscosity. *J. Fluid Mech.* 150: 451–65

Busse, F. H., Whitehead, J. A. 1971. Instabilities of convection rolls in a high Prandtl number fluid. *J. Fluid Mech.* 47: 305–20

Busse, F. H., Whitehead, J. A. 1974. Oscillatory and collective instabilities in large Prandtl number convection. *J. Fluid Mech.* 66: 67–80

Chandrasekhar, S. 1955. The character of the equilibrium of an incompressible heavy viscous fluid of variable density. *Proc. Cambridge Philos. Soc.* 51: 162–78

Cooper, R. F., Kohlstedt, D. L. 1984. Solution-precipitation enhanced diffusional creep of partially molten olivine-basalt aggregates. *Eos, Trans. Am. Geophys. Union* 65: 280 (Abstr.)

Crough, S. T. 1978. Thermal origin of mid-plate hot-spot swells. *Geophys. J. R. Astron. Soc.* 55: 451–69

Daněs, Z. F. 1964. Mathematical formulation of salt dome dynamics. *Geophysics* 29: 414–24

Dobrin, M. B. 1941. Some quantitative experiments on a fluid salt dome model and their geological implications. *Trans. Am. Geophys. Union* 22. 528–42

Emerman, S. H., Turcotte, D. L. 1983a. Stokes' problem with melting. *Int. J. Heat Mass Transfer* 26: 1625–30

Emerman, S. H., Turcotte, D. L. 1983b. Stagnation flow with a temperature-dependent viscosity. *J. Fluid Mech.* 127: 507–17

Epp, D. 1984. Implications of volcano and swell heights for thinning of the lithosphere by hot spots. *J. Geophys. Res.* 89: 9991–96

Fowler, A. C. 1984. On the transport of moisture in polythermal glaciers. *Geophys. Astrophys. Fluid Dyn.* 28: 99–140

Griffiths, R. W. 1986. Thermals in extremely viscous fluids, including the effects of temperature-dependent viscosity. *J. Fluid Mech.* 166: 115–38

Jackson, M. P. A., Talbot, J. C. 1986. External shapes, strain rates and dynamics of salt structures. *Geol. Soc. Am. Bull.* 97: 305–23

Krishnamurti, R. 1970. On the transition to turbulent convection, part 2. The transition to time-dependent flow. *J. Fluid Mech.* 42: 309 20

Loper, D. E., Stacey, F. D. 1983. The dynamical and thermal structure of deep mantle plumes. *Phys. Earth Planet. Inter.* 33: 304–17

Marsh, B. D. 1979. Island arc development: some observations, experiments and speculations. *J. Geol.* 87: 687–713

Marsh, B. D. 1982. On the mechanics of igneous diapirism, stoping and zone melting. *Am. J. Sci.* 282: 808–55

McKenzie, D. P. 1984. The generation and compaction of partial melts. *J. Petrol.* 25: 713–65

McKenzie, D. P., Weiss, N. O. 1975. Speculations on the thermal and tectonic history of the earth. *Geophys. J. R. Astron. Soc.* 42: 131–74

Morgan, W. J. 1971. Convection plumes in the lower mantle. *Nature* 230: 42–43

Morgan, W. J. 1972. Deep mantle convection plumes and plate motions. *Am. Assoc. Pet. Geol. Bull.* 56: 203–13

Morris, S. 1982. The effects of a strongly temperature-dependent viscosity on slow flow past a hot sphere. *J. Fluid Mech.* 124: 1–26

Nettleton, L. L. 1934. Fluid mechanics of salt domes. *Am. Assoc. Pet. Geol. Bull.* 18: 1175–1204

Nettleton, L. L. 1943. Recent experimental and geophysical evidence of mechanics of salt-dome formation. *Am. Assoc. Pet. Geol. Bull.* 27: 51–63

Oliver, D. S. 1980. *Bénard convection with strongly temperature-dependent viscosity.* PhD thesis. Univ. Wash., Seattle

Oliver, D. S., Booker, J. R. 1983. Planform of convection with strongly temperature-dependent viscosity. *Geophys. Astrophys. Fluid Dyn.* 27: 73–85

Olson, P., Singer, H. 1985. Creeping plumes. *J. Fluid Mech.* 158: 511–31

Olson, P., Nam, I. S. 1986. Formation of seafloor swells by mantle plumes. *J. Geophys. Res.* 91: 7181–91

Olson, P., Christensen, U. 1986. Solitary wave propagation in a fluid conduit within a viscous matrix. *J. Geophys. Res.* 91: 6367–74

O'Nions, R. K., Evenson, N. M., Hamilton, P. J. 1979. Geochemical modelling of mantle differentiation and crustal growth. *J. Geophys. Res.* 84: 6091–6101

O'Nions, R. K., Hamilton, P. R., Evenson, N. M. 1980. The chemical evolution of the earth's mantle. *Sci. Am.* 242: 120–33

Palm, E. 1960. On the tendency towards hexagonal cells in steady convection. *J. Fluid Mech.* 8: 183–92

Parker, T. J., McDowell, A. N. 1955. Model studies of salt-dome tectonics. *Am. Assoc. Pet. Geol. Bull.* 39: 2384–2470

Parmentier, E. M., Turcotte, D. L., Torrance, K. E. 1976. Studies of finite amplitude non-Newtonian thermal convection with application to convection in the earth's mantle. *J. Geophys. Res.* 81: 1839–46

Ramberg, H. 1963. Experimental study of gravity tectonics by means of centrifuged

models. *Bull. Geol. Inst. Univ. Uppsala* 42: 1–97
Ramberg, H. 1967a. Model experimentation of the effect of gravity on tectonic processes. *Geophys. J. R. Astron. Soc.* 14: 307–29
Ramberg, H. 1967b. *Gravity Deformation and the Earth's Crust as Studied by Centrifuged Models.* Orlando, Fla: Academic. 224 pp.
Ramberg, H. 1968a. Fluid dynamics of layered systems in a field of gravity, a theoretical basis for certain global structures and isostatic adjustment. *Phys. Earth Planet. Inter.* 1: 63–87
Ramberg, H. 1968b. Instability of layered systems in a field of gravity, 1, 2. *Phys. Earth Planet. Inter.* 1: 427–74
Ramberg, H. 1968c. Mantle diapirism and its tectonic and magmagenetic consequences. *Phys. Earth Planet. Inter.* 5: 45–60
Ramberg, H. 1970. Model studies in relation to intrusion of plutonic bodies. *Geol. J. Spec. Issue* 2: 261–86
Rayleigh, Lord. 1900. Investigation of the character of the equilibrium of an incompressible heavy fluid of variable density. In *Scientific Papers of Lord Rayleigh*, 2: 200–7. New York: Dover (1964)
Ribe, N. M. 1983. Diapirism in the Earth's mantle: experiments on the motion of a hot sphere in a fluid with temperature dependent viscosity. *J. Volcanol. Geotherm. Res.* 16: 221–45
Ribe, N. M. 1985. The generation and compaction of partial melts in the earth's mantle. *Earth Planet. Sci. Lett.* 73: 361–76
Richter, F. M. 1978a. Mantle convection models. *Ann. Rev. Earth Planet. Sci.* 6: 9–19
Richter, F. M. 1978b. Experiments on the stability of convection rolls in fluids whose viscosity depends on temperature. *J. Fluid Mech.* 89: 553–60
Richter, F. M., McKenzie, D. 1984. Dynamical models for melt segregation from a deformable matrix. *J. Geol.* 92: 729–40
Richter, F. M., Parsons, B. 1975. On the interaction of two scales of convection in the mantle. *J. Geophys. Res.* 80: 2529–41
Schouten, H., Whitehead, J. A., Klitgord, K. D. 1985. Segmentation of mid-ocean ridges. *Nature* 317: 225–29
Scott, D. R. 1987. *Magmons: solitary waves arising in the buoyant ascent of magma by porous flow through a viscously deformable matrix.* PhD thesis. Calif. Inst. Technol., Pasadena
Scott, D. R., Stevenson, D. J. 1984. Magma solitons. *Geophys. Res. Lett.* 11: 1161–64
Scott, D. R., Stevenson, D. J. 1986. Magma ascent by porous flow. *J. Geophys. Res.* 91: 9283–96
Scott, D. R., Stevenson, D. J., Whitehead, J. A. 1986. Observations of solitary waves in a viscously deformable pipe. *Nature* 319: 759–60
Segel, L. A., Stuart, J. T. 1962. On the question of preferred mode in cellular thermal convection. *J. Fluid Mech.* 13: 289–306
Selig, F. 1965. A theoretical prediction of salt dome patterns. *Geophysics* 30: 633–43
Skilbeck, J. N., Whitehead, J. A. Jr. 1978. Formation of discrete islands in linear island chains. *Nature* 272: 499–501
Stacey, F. D. 1977. A thermal model of the earth. *Phys. Earth Planet. Inter.* 15: 341–48
Stacey, F. D., Loper, D. E. 1983. The thermal boundary layer interpretation of *D″* and its role as a plume source. *Phys. Earth Planet. Inter.* 33: 45–55
Stuart, J. T. 1964. On the cellular patterns in thermal convection. *J. Fluid Mech.* 18: 481–98
Von Herzen, R. P., Detrick, R. S., Crough, S. T., Epp, D., Fehn, U. 1982. Thermal origin of the Hawaiian swell: heat flow evidence and thermal models. *J. Geophys. Res.* 87: 6711–23
Waff, H. S. 1980. Effects of the gravitational field on liquid distribution in partial melts within the upper mantle. *J. Geophys. Res.* 85: 1815–25
Waff, H. S., Bulau, J. R. 1979. Equilibrium in fluid distribution in partial melts under hydrostatic stress conditions. *J. Geophys. Res.* 84: 6109–14
White, D. B. 1982. *Experiments with convection in a variable viscosity fluid.* PhD thesis. Univ. Cambridge, Engl.
Whitehead, J. A. Jr. 1982. Instabilities of fluid conduits in a flowing earth—are plates lubricated by the asthenosphere? *Geophys. J. R. Astron. Soc.* 70: 415–33
Whitehead, J. A. 1986. Buoyancy-driven instabilities of low-viscosity zones as models of magma-rich zones. *J. Geophys. Res.* 91: 9303–14
Whitehead, J. A. 1987. Solitary waves in a vertical conduit in syrup: the possibility of laboratory solitons. *Am. J. Phys.* In press
Whitehead, J. A., Luther, D. S. 1975. Dynamics of laboratory diapir and plume models *J. Geophys. Res.* 80: 705–17
Whitehead, J. A., Chan, G. 1976. Stability of Rayleigh-Bénard convection rolls and bimodal flow at moderate Prandtl number. *Dyn. Atmos. Oceans* 1: 33–49
Whitehead, J. A., Parsons, B. 1978. Observations of convection at Rayleigh numbers up to 760,000 in a fluid with large Prandtl number. *Geophys. Astrophys. Fluid Dyn.* 9: 201–17
Whitehead, J. A. Jr., Dick, H. J. B.,

Schouten, H. 1984. A mechanism for magmatic accretion under spreading centers. *Nature* 312: 146–48

Whitehead, J. A., Helfrich, K. R. 1986. The Korteweg–de Vries equation from laboratory conduit and magma migration equations. *Geophys. Res. Lett.* 13: 545–46

Wilson, J. T. 1963. A possible origin of the Hawaiian islands. *Can. J. Phys.* 41: 863–70

Yuen, D. A., Peltier, W. R. 1980a. Mantle plumes and the thermal stability of the *D″* layer. *Geophys. Res. Lett.* 7: 625–28

Yuen, D. A., Peltier, W. R. 1980b. Temperature-dependent viscosity and local instabilities in mantle convection. In *Physics of the Earth's Interior*, ed. A. Dziewonski, E. Boschi, pp. 432–63. Amsterdam: North-Holland

Yuen, D. A., Schubert, G. 1976. Mantle plumes: a boundary layer approach for Newtonian and non-Newtonian temperature-dependent rheologies. *J. Geophys. Res.* 81: 2499–2510